University of Twente

Faculty of
Mechanical Engineering

Applied Mechanics

APPLICATION AND EXPERIMENTAL VERIFICATION OF DIANA FOR ACOUSTO-ELASTIC PROBLEMS

WB.96/TM-1523

This paper has been prepared for presentation at the
First International DIANA Conference on Computational
Mechanics 1994 Delft The Netherlands

by

W.M. Beltman, P.J.M. van der Hoogt,
R.M.E.J. Spiering, H. Tijdeman

APPLICATION AND EXPERIMENTAL VERIFICATION OF DIANA FOR ACOUSTO-ELASTIC PROBLEMS

W.M. Beltman, P.J.M. van der Hoogt, R.M.E.J. Spiering and H. Tijdeman
University of Twente
Department of Mechanical Engineering
Applied Mechanics
P.O. Box 217
7500 AE Enschede
The Netherlands

Abstract. The coupling between a vibrating structure and the surrounding compressible fluid was established by modification of an existing DIANA element. Calculations and experiments were carried out for air in a closed box with a flexible coverplate. The influence of the cavity depth on the eigenfrequencies and mode shapes of the plate was investigated. Calculations and experiments show good agreement. For small depths however viscous effects have to be taken into account.

1. Introduction

In most vibration calculations the influence of the surrounding fluid on a vibrating structure is neglected. When the structure however is relatively light and flexible the effect of the surrounding fluid has to be taken into account. For these cases a fluid-structure interaction calculation has to be carried out. In an interaction calculation the noise levels can be predicted. Using this technique it is possible to reduce the interior noise levels in for instance cabins of passenger cars. A short introduction in the acousto-elastic theory will be given in section 2. In section 3 an application is described. Calculations and experiments are compared and a physical interpretation of the phenomena is given. The conclusions are presented in section 4.

2. Acousto-Elastic Calculations in DIANA

In interaction problems three types of vibration modes can be distinguished: structural modes, acoustic modes and coupled modes. The structural modes are the modes of the structure in vacuum. The acoustic modes are the modes of the fluid when all the walls are assumed to be rigid. For the coupled, or acousto-elastic modes the mutual interaction between the vibrating structure and the surrounding fluid is taken into account. All three types of modes can be calculated with the finite element method. The structure is modelled using solid or plate elements. The resulting set of equations for the structural vibrations is written as:

$$[M_s]\{\ddot{U}\} + [C_s]\{\dot{U}\} + [K_s]\{U\} = \{F_s\} \qquad (1)$$

The structural modes and frequencies are obtained from the corresponding eigenvalue problem by choosing $\{F_s\}$ equal to zero.

The fluid is represented as a compressible inviscid medium with no mean flow. For this case the behaviour of the fluid can be described with the wave equation:

$$\nabla^2 p = \frac{1}{c^2}\frac{\partial^2 p}{\partial t^2} \qquad (2)$$

where p is the pressure perturbation and c is the speed of sound. This equation is used to set up the finite element equations for the fluid part:

$$[M_f]\{\ddot{P}\} + [C_f]\{\dot{P}\} + [K_f]\{P\} = \{F_f\} \qquad (3)$$

The acoustic modes and frequencies can be calculated from the corresponding eigenvalue problem by choosing $\{F_f\}$ equal to zero. An acoustic finite element implemented in DIANA by modification of an existing fluid element.
The new element is a 4-node linear fluid element, Q4HT, with the pressure perturbation as the degree of freedom at each node (see figure 1). A number of tests are carried out for this element and the results are compared with analytical solutions [6]. These modifications are extended to other elements, *e.g.* the 8-node CHX60H element. The coupling between a vibrating structure and the surrounding fluid is established by demanding continuity of velocity across the fluid-structure interface. The motion of the structure has to be followed by the fluid, while the fluid pressure serves as an excitation for the structure. Using these interface conditions, elements of the structure can be coupled to the new fluid elements (see figure 2). In DIANA the coupling is realized with the generalized interface element FSELM and the appropriate interface element. The displacements of the fluid nodes on the interface are coupled to the displacements of the structure. This mutual interaction can be expressed in terms of the acousto-elastic equations:

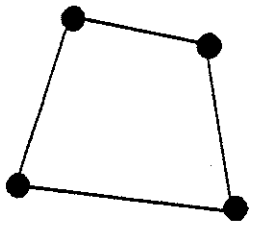

Fig 1: Q4HT element

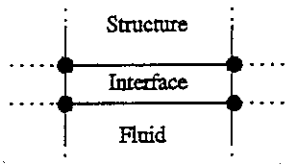

Fig 2: Interface

$$\begin{bmatrix} [M_s] & [0] \\ [M_c] & [M_f] \end{bmatrix} \begin{Bmatrix} \{\ddot{U}\} \\ \{\ddot{P}\} \end{Bmatrix} + \begin{bmatrix} [C_s] & [0] \\ [0] & [C_f] \end{bmatrix} \begin{Bmatrix} \{\dot{U}\} \\ \{\dot{P}\} \end{Bmatrix} + \begin{bmatrix} [K_s] & -[K_c] \\ [0] & [K_f] \end{bmatrix} \begin{Bmatrix} \{U\} \\ \{P\} \end{Bmatrix} = \begin{Bmatrix} \{F_s^{ext}\} \\ \{F_f^{ext}\} \end{Bmatrix} \qquad (4)$$

where the index c refers to coupling and:

$$[M_c] = \rho_f c^2 [K_c]^T \qquad (5)$$

where ρ_f is the fluid density. The resulting set of equations forms a coupled asymmetric system. The coupling is expressed by the coupling matrices $[M_c]$ and $[K_c]$. At the time of writing an appropriate eigensolver was missing in DIANA 5.1 and the coupled eigenfrequencies still had to be calculated using the direct method.

3. Application and Experimental Verification

3.1 Formulation of the Problem

In order to investigate the effects of a fluid filled cavity on the vibrational behaviour of a plate, calculations and experiments were carried out for an airtight box with a flexible coverplate (see figure 3). This experiment was described in reference [2].

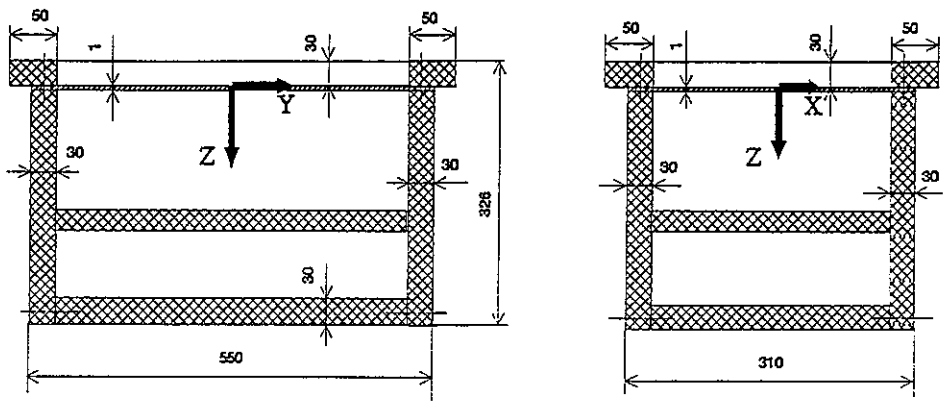

Fig 3: Airtight box with flexible coverplate; measures in mm

An aluminium plate was clamped in a perspex (PMMA) box. The cavity depth could be varied using a movable bottom plate (see figure 3). The eigenfrequencies and the mode shapes of the plate were investigated as a function of the depth of the cavity. The experimental setup is depicted in figure 4.

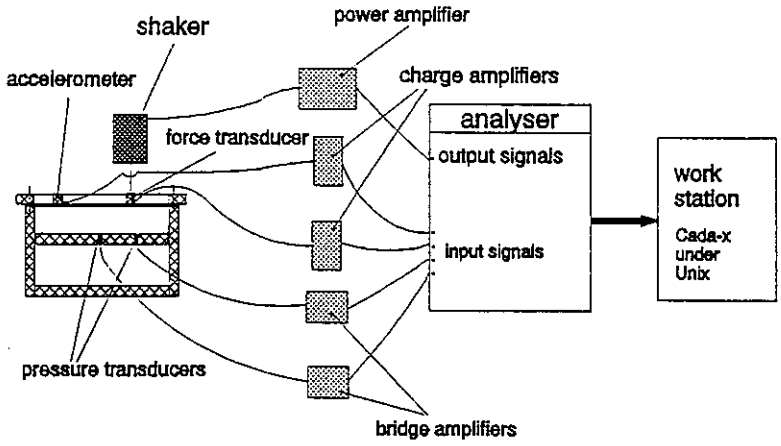

Fig 4: Experimental setup

The plate was excited by an electrodynamic shaker. The excitation signal was a noise signal in the frequency range of interest, *i.e.* 64-576 Hz. The response was measured with an accelerometer. In order to obtain the mode shapes the response was sequentially measured in seven different points on the plate. Due to the difference in thermal expansion coefficients between the perspex and the aluminium the experiments were carried out under controlled climatic conditions [4].

3.2 Structural Modes

The structural modes were calculated using the quadratic shell element CQ40F. Symmetry and anti-symmetry conditions were imposed in order to reduce the model to one quarter of the plate. The mesh contained 3x4 elements (see figure 5)
Material properties:

$\rho_s = 2700\ kg/m^3$

$h = 1\ mm$

$E = 70 \cdot 10^9\ N/m^2$

$\nu = 0.3$

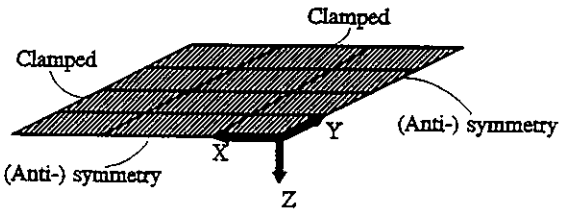

Fig 5: Plate elements

A 2x2 integration scheme was used.
The shear factor for the plate elements was calculated using the element surface A and the plate thickness h according to [7]:

$$k = 1 + \frac{0.2A}{25h^2} \qquad (6)$$

The structural modes were identified by the number of half wave lengths in the x and y direction respectively. The results from the DIANA calculations were in reasonable agreement with analytical results [1] as can be seen from table I.
The first three mode shapes of the entire plate are given in the figures 6, 7 and 8.

Table I
Eigenfrequencies of the plate

Mode	Eigenfrequency (Hz) DIANA 5.1	Analytical
f_{11}	97.0	96.3
f_{12}	128.3	126.5
f_{13}	186.2	180.2
f_{21}	252.3	251.8
f_{14}	269.4	256.9
f_{22}	285.4	281.6

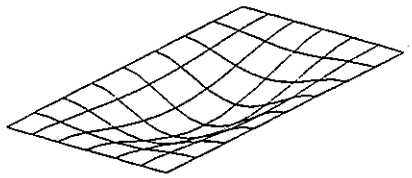

Fig 6: First structural mode

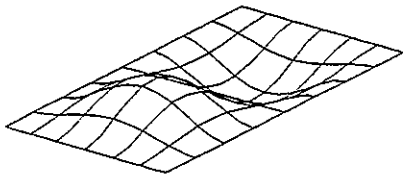

Fig 7: Second structural mode

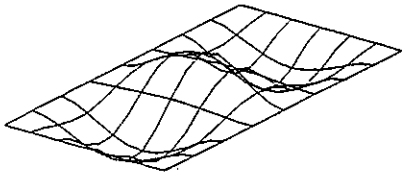

Fig 8: Third structural mode

3.3 Acoustic Modes

The acoustic modes for the complete cavity were calculated with the help of the new quadratic fluid element CHX60H. Symmetry and anti-symmetry conditions were imposed in order to reduce the model to one quarter of the fluid domain (see figure 9). The mesh contained 3x4x3 elements.
Material properties of the air:

$$c = 340\ m/s$$

$$\rho_f = 1.2\ kg/m^3$$

A 2x2x2 integration scheme was used. The boundary condition for all surfaces were:

$$\frac{\partial p}{\partial n} = 0 \qquad (7)$$

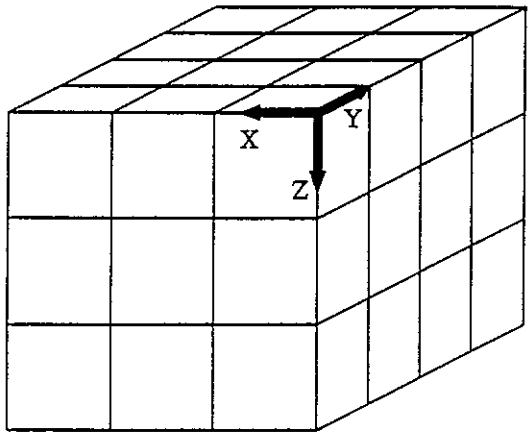

Fig 9: Fluid elements

where n is normal to the surface.
This condition was automatically satisfied in the calculation when no other boundary conditions were applied.
The acoustic modes were identified by the number of half wave lengths in the x, y and z direction respectively. The pressure distribution for the first mode is given in figure 10. An analytical solution can easily be obtained for this case [4]. As can be seen from table II, DIANA results showed fair agreement with the analytical results.

Table II
Eigenfrequencies of the acoustic domain

Mode	Eigenfrequency (Hz) DIANA 5.1	Analytical
f_{010}	347.0	346.9
f_{001}	640.1	639.1
f_{100}	680.1	680.0
f_{020}	694.2	693.9
f_{011}	728.1	727.2

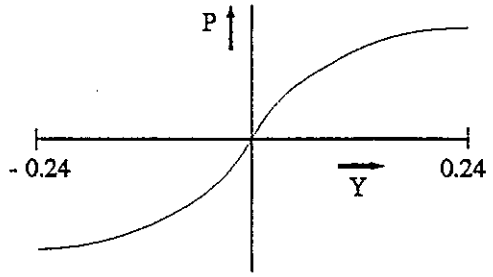

Fig 10: First acoustic mode

3.4 Acousto-Elastic Modes

The acousto-elastic calculations were carried out for different values of the cavity depth. The interaction between the plate and the fluid was established using the generalized interface element FSELM and the quadratic interface element BQ24S8. Again, symmetry and anti-symmetry conditions were imposed in order to reduce the model to one quarter of the fluid-plate system. The walls of the perspex cavity were assumed to be rigid. The influence of the fluid on the upper side of the plate is negligible for the frequency range of interest [1]. The number of elements in x, y and z direction for each cavity depth is given is table III. The elements are depicted in figure 11.

Table III
Elements in cavity mesh

depth (mm)	elements
266, 150	3x4x3
100, 60, 50, 30	3x4x2
25, 20, 10, 5	3x4x1

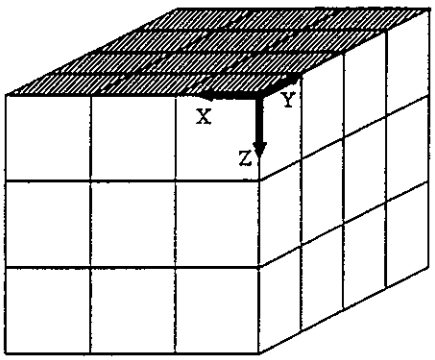

Fig 11: Coupled elements

The eigenfrequencies and the corresponding mode shapes for the first three coupled modes were calculated for all cavity depths. The results of the numerical calculations with DIANA were in good agreement with experimental results, as can be seen from figure 12.

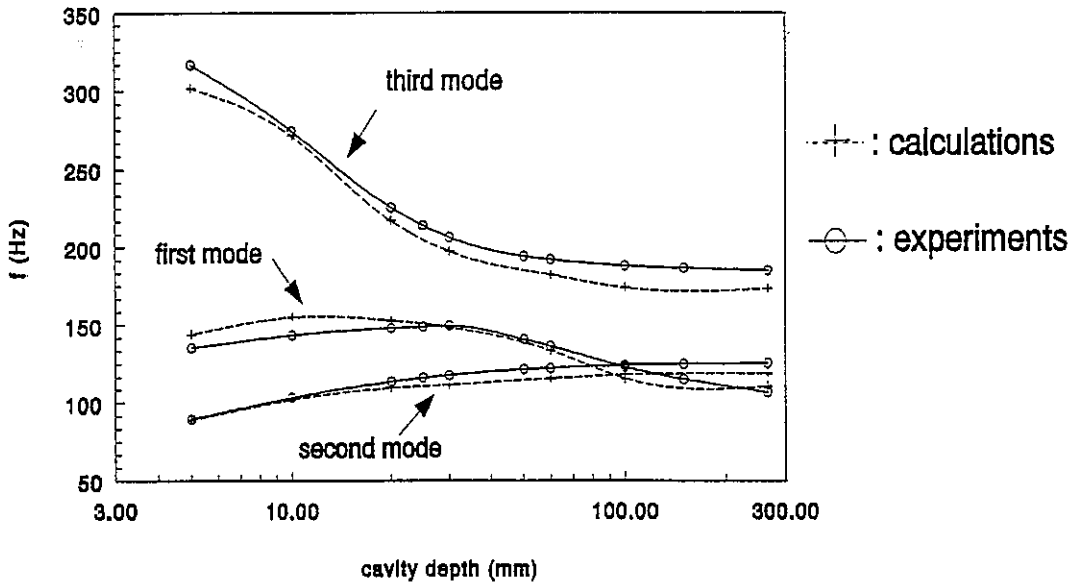

Fig 12: Coupled eigenfrequencies for varying cavity depth

For the first three modes there was a significant shift in eigenfrequency when the depth of the cavity was varied. The calculated mode shapes in the y direction for the first three modes for depths of 266 mm, 50 mm and 10 mm are given in the figures 13, 14 and 15. In all cases a good agreement between computations and experiments was obtained. The mentioned figures reveal a dramatic change in mode shapes when the depth of the cavity is varied, especially for the first and the third mode. A physical interpretation for these phenomena will be given in the next section.

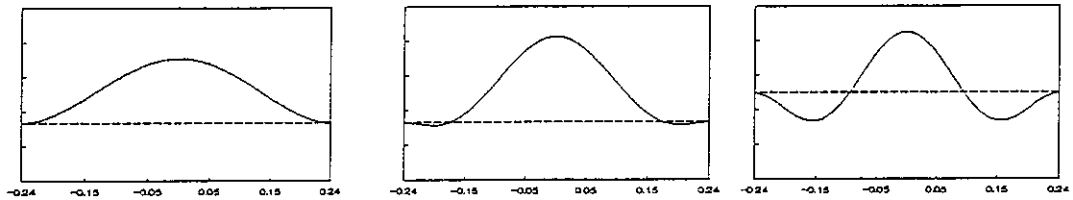

Fig 13: Shape of the first mode

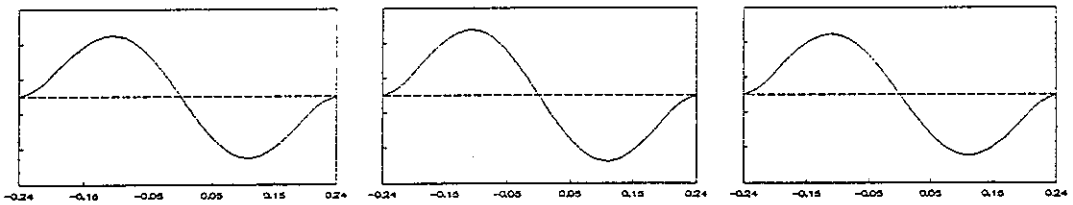

Fig 14: Shape of the second mode

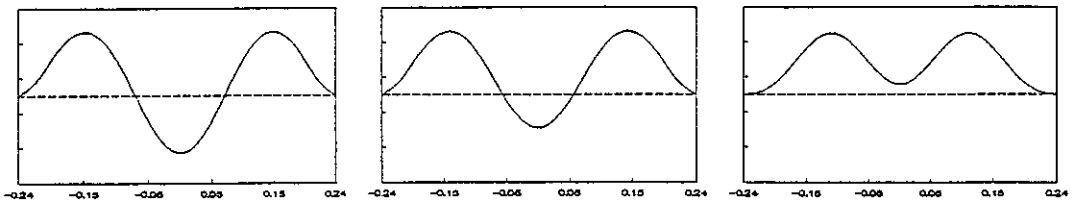

Fig 15: Shape of the third mode

3.5 Physical Interpretation

Figure 12 learns that the eigenfrequency of the first mode increases with decreasing cavity depth in the range between 266 and 30 mm., while the second mode shows a decrease in eigenfrequency with decreasing cavity depth. Below a depth of 30 mm. the eigenfrequency of the first mode however decreases with decreasing depth. The frequency of the third mode increases with decreasing depth of the cavity. This behaviour can be explained by a consideration of the added mass and the added stiffness [4].

Added mass

In general a vibrating structure experiences the motion of the surrounding fluid as if it possessed an extra mass. For a plate vibrating in an infinite fluid domain, exact solutions for the added mass are known [1]. In this case however the fluid is trapped in a cavity. It turns out that the added mass effect for this situation increased with decreasing cavity depth. This is especially the case for the second mode. This is not too surprising because for this mode the fluid in the cavity has to move periodically back and forth in a direction which is mainly perpendicular to the motion of the plate, as depicted in figure 16. Due to this 'pumping', the plate experiences a stong added mass effect, resulting in a drop in eigenfrequency. For small cavity depths the first mode changes to a shape which also induces a pumping effect (see figure 13). Therefore the eigenfrequency of the first mode also decreased for cavity depths below 30 mm.

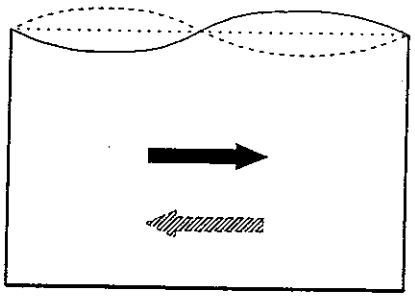

Fig 16: Pumping effect in the second mode

Added stiffness

The added mass effect is in contradiction with the observation that the eigenfrequencies of the first and the third mode shows an increase with decreasing cavity depth. This increase in eigenfrequency can be explained as follows. The first and the third mode are symmetric modes (see figures 13 and 15) and for these modes the deformation of the coverplate is accompanied by a significant change in volume in the cavity (see left hand side of figure 17).

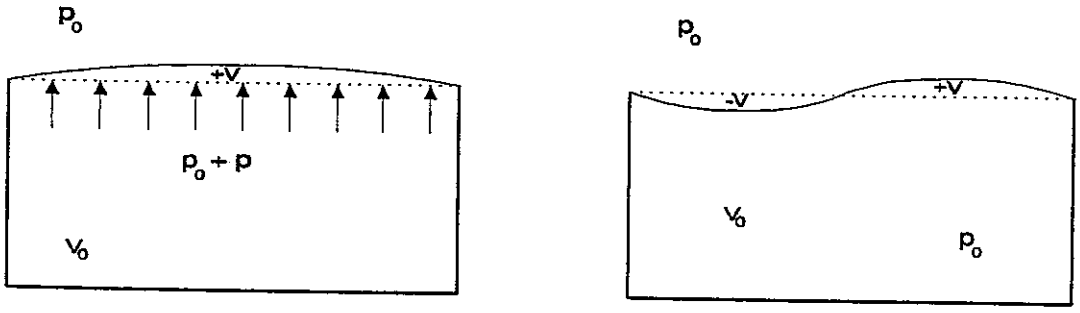

Fig 17: Change in cavity volume for the first and the second mode

Due to the change in volume the pressure in the cavity changes. If we assume that the process is quasi-stationary and that the change in pressure is equal everywhere in the cavity, the pressure perturbation in the cavity can be obtained from:

$$p_0 V_0 = (p_0 + p)(V_0 + V) \tag{8}$$

Neglecting higher order terms gives:

$$p = -p_0 \frac{V}{V_0} \tag{9}$$

The load acting on the plate due to this pressure disturbance is in phase with the motion of the plate. Therefore the plate experiences this load as an added stiffness and the eigenfrequency will increase. As can be seen from equation 9 the pressure disturbance, and therefore also the added stiffness, increases with decreasing cavity depth. The added stiffness effect also causes a dramatic change in mode shape, as can be seen in the figures 13 and 15. The second mode is an asymmetric mode that does not create a change of cavity volume (see right hand side of figure 17). Therefore this mode does not experience an added stiffness effect. This mode only experiences an added mass effect: the eigenfrequency drops with decreasing depth. The first mode is a symmetric mode. In the depth range of 266 downto 30 mm. the added stiffness effect dominates the added mass effect and the eigenfrequency increases with decreasing cavity depth. For depths below 30 mm. the shape of the mode has changed in such a way that the added mass now dominates and the eigenfrequency drops with decreasing cavity depth. For the third mode the added stiffness effect dominates and the eigenfrequency increases with decreasing depth.

Viscosity

Care has to be taken when the cavity depth is very small. The experiments showed a significant increase in damping for this situation, especially for the second mode. The extra damping is due to the viscosity of the air: the pumping effect in the second mode induces significant viscous losses. In figure 18 the damping coefficient for the first three modes is given for a number of cavity depths. The damping for the first and the third mode is very low in comparison with damping for the second mode, due to the absence of a pumping effect for these modes. It can be shown that for narrow gaps the viscous effects are of the same order of magnitude as the inertia effects [3,5]. It is evident that in these situations the assumptions on which the wave equation is based are no longer valid.

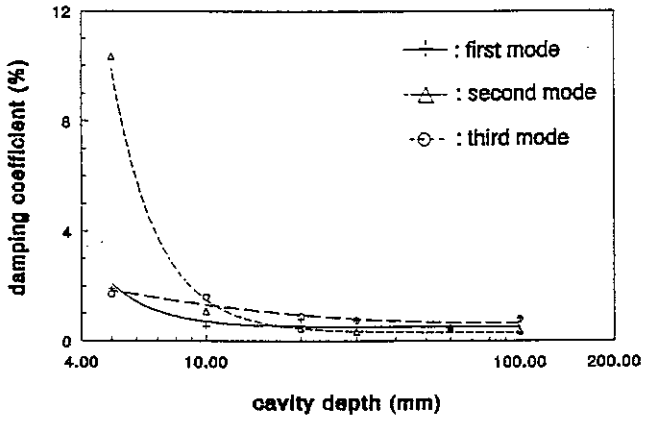

Fig 18: Damping coefficients

4 Conclusions

DIANA has been extended with the possibility to take account of the coupling between a vibrating structure and the surrounding compressible fluid. The structural and acoustic modes computed with DIANA for an airtight box showed good agreement with analytical results. The results from the interaction calculation were in close agreement with the experimental results. During the experiments some interesting phenomena have been observed which could be predicted very well. For very small gaps the viscosity of the fluid plays an important role. This effect is still beyond the possibilities of DIANA.

References

1. Blevins, R.D., *Formulas for natural frequency and mode shape*, Van Nostrand Reinholds company, New York, 1979
2. Dowell, E.H., Gorman, G.F. and Smith, D.A., *Acousto-elasticity: generaltheory, acoustic natural modes and forced response to sinusoidal excitation, including comparisons with experiment*, Journal of Sound and Vibration, Vol.52, p.519-542, 1977
3. Fox, M.J.H. and Whitton, P.N., *The damping of structural vibration by thin gas films*, Journal of Sound and Vibration, Vol.73(2), p.279-295, 1980
4. Luyten, J.M., *Interactie tussen een akoestisch drukveld en een flexibele structuur*, University of Twente, 1993
5. Önsay, T., *Effects of layer thickness on the vibration response of a plate-fluid layer system*, Journal of Sound and Vibration, Vol.163(2), p.231-259, 1993
6. Veen, B. van, *Akoestische berekeningen met de eindige elementen methode*, WB.92/TM-335, University of Twente, 1992
7. Vries, S. de, *Voortgaande ontwikkeling van eindige-elementen voor visco-elastische laminaatplaten*, WB.93/TM-545, University of Twente, 1992

List of Symbols

Symbols:

A	surface
c	speed of sound
E	Young's modulus
f	frequency
h	plate thickness
k	shear factor
n	normal on the surface
p	pressure perturbation
t	time
V	volume
ν	Poisson's ratio
ρ	density

Operators:

$\dot{}$	time derivative
∇	gradient operator
∂	partial derivative

Matrices and vectors:

[M]	mass matrix
[C]	damping matrix
[K]	stiffness matrix
{F}	nodal force vector
{P}	nodal pressure perturbation vector
{U}	nodal displacement vector

Superscripts and subscripts:

^{c}	refers to coupled
$_{ext}$	external
$_f$	refers to fluid
$_s$	refers to structure
$_0$	mean value